

## Tau-4R suppresses proliferation and promotes neuronal differentiation in the hippocampus of tau knockin/knockout mice

Kristina Sennvik,<sup>\*,1</sup> Karin Boekhoorn,<sup>†,1</sup> Reena Lasrado,<sup>\*,1</sup> Dick Terwel,<sup>\*</sup> Steven Verhaeghe,<sup>\*</sup> Hubert Korr,<sup>‡</sup> Christoph Schmitz,<sup>‡</sup> Takami Tomiyama,<sup>§</sup> Hiroshi Mori,<sup>§</sup> Harm Krugers,<sup>†</sup> Marian Joels,<sup>†</sup> Ger J. A. Ramakers,<sup>||</sup> Paul J. Lucassen,<sup>†</sup> and Fred Van Leuven<sup>\*,2</sup>

<sup>\*</sup>Experimental Genetics Group, Department Human Genetics, K.U.Leuven, Leuven, Belgium;

<sup>†</sup>Section Neurobiology, Swammerdam Institute of Life Sciences, Amsterdam, The Netherlands;

<sup>‡</sup>Department of Anatomy and Cell Biology, Rheinland-Westfalen Technischen Hochschule University of Aachen, Aachen, Germany; <sup>§</sup>Department of Neuroscience, Medical School, Osaka, Japan; and

<sup>||</sup>Netherlands Institute for Brain Research, Amsterdam, The Netherlands

**ABSTRACT** Differential isoform expression and phosphorylation of protein tau are believed to regulate the assembly and stabilization of microtubuli in fetal and adult neurons. To define the functions of tau in the developing and adult brain, we generated transgenic mice expressing the human tau-4R/2N (htau-4R) isoform on a murine tau null background, by a knockout/knockin approach (tau-KOKI). The main findings in these mice were the significant increases in hippocampal volume and neuronal number, which were sustained throughout adult life and paralleled by improved cognitive functioning. The increase in hippocampal size was found to be due to increased neurogenesis and neuronal survival. Proliferation and neuronal differentiation were further analyzed in primary hippocampal cultures from tau-KOKI mice, before and after htau-4R expression onset. In absence of tau, proliferation increased and both neurite and axonal outgrowth were reduced. Htau-4R expression suppressed proliferation, promoted neuronal differentiation, and restored neurite and axonal outgrowth. We suggest that the tau-4R isoform essentially contributes to hippocampal development by controlling proliferation and differentiation of neuronal precursors.—Sennvik, K., Boekhoorn, K., Lasrado, R., Terwel, D., Verhaeghe, S., Korr, H., Schmitz, C., Tomiyama, T., Mori, H., Krugers, H., Joels, M., Ramakers, G. J. A., Lucassen, P. J., Van Leuven, F. Tau-4R suppresses proliferation and promotes neuronal differentiation in the hippocampus of tau knockin/knockout mice. *FASEB J.* 21, 2149–2161 (2007)

*Key Words:* transgenic mice • neurogenesis • cognition • primary cultures

PROTEIN TAU IS A MAJOR MICROTUBULE associated protein (MAP) in the vertebrate nervous system. In human brain, six tau isoforms are generated from a

single gene through alternative mRNA splicing (reviewed in (1–3)). The isoforms differ by having none, one or two N-terminal inserts and either three or four C-terminal microtubule binding repeat domains. The three-repeat (3R) tau isoform predominates in early developmental stages in both humans and rodents. But whereas tau-3R and tau-4R levels are about equal in adult human brain, a practically complete switch to tau-4R expression occurs in rodent brain after the second postnatal week (4–6).

The biological significance of differential tau isoform expression may be inferred from their respective regulation during development and from the role of tau-4R in the neurodegenerative disorders known as tauopathies. Of particular interest are the familial forms of frontotemporal dementia (FTD), caused by intronic tau mutations that result in perturbed tau isoform ratios rather than expression of mutant tau. FTD and many different neurodegenerative diseases that manifest late in life are characterized by neurofibrillar inclusions of highly phosphorylated protein tau (2, 7).

Transgenic mouse strains expressing human tau have previously been generated to study the function of wild-type and mutant tau and their contributions toward tauopathy and neurodegeneration (7). Expression of human tau (htau) by a genomic DNA construct on a null tau murine background resulted in progressive hyperphosphorylation and tau aggregation in aged mouse brain (6). On the other hand, expression of human tau-4R (htau-4R) or htau-4R(P301L) on a murine tau background have been shown to cause mutually exclusive pathologies in a dose-dependent manner

<sup>1</sup> These authors contributed equally to this work.

<sup>2</sup> Correspondence: Experimental Genetics Group, Department Human Genetics, KULeuven - Campus Gasthuisberg ON1-06.602, B-3000 Leuven, Belgium. E-mail: fredvl@med.kuleuven.be

doi: 10.1096/fj.06-7735com

(8, 9). Both gene dosage and tau isoform ratios may thus influence pathology.

In this study, we describe a simplified mouse model, wherein the endogenous murine tau gene has been inactivated and replaced by a single copy of the htau-4R/2N isoform (knockin/knockout). The mice express htau-4R at physiological levels, allowing us to study isoform specific functions of tau-4R in neurodevelopment and disease.

## MATERIALS AND METHODS

### Generation of transgenic mice

The tau knockout/knockin strain of htau-4R (tau-KOKI) was engineered to inactivate the endogenous murine tau gene and to replace it with a single copy of the thyl-htau-4R/2N recombinant DNA construct (8, 9). The excised insert was ligated in the *Bam*HI site of the pBluescript vector, followed by ligation into a unique *Sma*I site of a 1.9 kb *Not*I fragment encoding the hygromycin B phosphotransferase gene driven by the phosphoglycerate kinase promoter (10). The total insert of this construct was excised to remove vector sequences and ligated in the unique *Nco*I site in exon1 of the mouse tau gene, partially subcloned from the 129 mouse strain (11). The targeting vector was linearized by *Not*I restriction and electroporated into embryonic stem (ES) cells that were cultured and genotyped as in (12). ES cells were microinjected into 4 d old blastocysts from C57/Bl6 mice. Reimplantation into pseudo-pregnant CD1 females resulted in coat-color chimeras, proving germline transmission. Chimeric offspring were crossed with FVB/N mice and genotyped.

### Stereological analysis

Total numbers of cells in specified brain regions were quantified in 30  $\mu$ m sagittal cryostat sections stained with cresyl violet. Every 10th section was analyzed in a series of systematically sampled hippocampal sections that totaled 10–15 sections per brain. For each genotype, 7 mice at age 6 mo were analyzed.

Neuronal number quantification was performed by estimating the volume of the region through the point-counting method and Cavalieri's principle. Neurons were counted by registering cells within three-dimensional optical dissectors systematically and randomly spaced throughout the region. Unbiased neuron number estimates were obtained from the cell counts using the fractionator principle (13). Stereological analysis was performed on a stereology system (CAST-Grid; Olympus, Glostrup, Denmark) consisting of a microscope, motorized specimen stage, microcator, CCD video camera, computer, and stereology software (14). Postprocessing section thickness was measured at each dissector location. Cells with typical neuronal morphology, including clearly delineated nucleolus, were counted within the optical dissector frame at  $\times 100$ . For hippocampal pyramidal cells, borders were evident between subiculum and dentate gyrus cells. Hippocampal granular cells were clearly delineated in and from the molecular and hilar regions of the dentate gyrus. Statistical analyses were carried out with GraphPad Prism 3.0 (GraphPad Software, San Diego, CA, USA).

### Behavioral testing

At 5 and 9 wk of age, mice were subjected to behavioral tests. General motor ability was assessed by rotarod testing, using a

revolving, horizontal rod of 3.2 cm diameter (Med Associates, Georgia, Vermont, USA). After one (5-wk-old mice) or two (9-wk-old mice) training sessions of 5 min at 16 revolutions per minute (rpm), the mice were placed on the rod, and the speed was increased from 4 to 40 rpm over 3 min. The time that the mice stayed on the rod was recorded.

Exploratory and motor activities were determined in an open field setting. Each mouse was placed for 5 min on an elevated, white opaque plastic surface of 52  $\times$  52 cm without bordering walls. The travel path was recorded and analyzed using dedicated software (Ethovision-Noldus, The Netherlands). The center of the open field was defined as an inner square of 40  $\times$  40.

Hippocampus-dependent learning and memory were analyzed using the novel object recognition test (NORT), as described previously (12). Individual mice were habituated on day 1 for 2  $\times$  5 min in a box (52 $\times$ 52 $\times$ 40 cm), with black walls and a white opaque floor illuminated from below. On day 2, mice were familiarized for 10 min with two identical objects placed in adjacent quadrants of the box. Travel paths and the time the mice spent exploring an object with its snout directed toward the object within nostril reach were recorded. In the memory retention trial of 10-min duration, the mice were tested with one familiar and one novel object after a delay of either 1 or 3.5 h. The novel object and its position were randomized to avoid preferences not based on novelty. The level of discrimination ( $d_2$ ) was defined as  $d_2 = (b-a)/(b+a)$ , wherein a and b are the exploration times spent on old and novel objects. Statistical analyses were performed with 2-way ANOVA.

### Electrophysiological analysis

Mice were decapitated, brains were removed, and kept at 4°C in artificial cerebrospinal fluid (ACSF) as described by Boekhoorn et al. (15). For Schaffer collateral recordings, 400  $\mu$ m transversal hippocampal sections were cut with a tissue chopper; for perforant path recordings, 400- $\mu$ m horizontal fore-brain sections were cut with a vibroslicer. After 1 h of incubation at room temperature in oxygenated recording ACSF, slices were transferred to a recording chamber and perfused with oxygenated ACSF at 31.5°C. Bipolar stimulating electrodes isolated with stainless steel were placed in the Schaffer collaterals or the perforant path to record field excitatory postsynaptic potentials (fEPSPs) using a glass microelectrode (2–5 M $\Omega$  filled with ACSF) placed in the stratum radiatum of the CA1 or the middle third of the molecular layer of the DG. To evoke robust LTP in the DG, GABA-mediated activity was blocked with 10- $\mu$ M bicuculline methiodide (Sigma, St. Louis, MO, USA) in the ACSF. Before baseline recording, the maximal fEPSP amplitude and slope were determined by increasing the stimulus intensity until the response was saturated. The relationship between the stimulus intensity and the evoked response was fit to a Boltzmann equation:  $R_{(i)} = R_{max}/(1 + \exp(-(I - i_h)/S))$ , wherein  $R_{(i)}$  is the response at stimulus intensity ( $i$ ),  $R_{max}$  is the maximal response,  $i_h$  is the intensity at which the half-maximal response is observed and slope factor  $S$  is the index that describes the slope of the stimulus-response curve.  $i_h$  was used to record baseline responses for at least 20 min. Paired-pulses with interstimulus intervals of 50, 100, 200, and 500 ms were tested in the DG to make sure the medial perforant path was stimulated. LTP was evoked in the CA1 and the DG, using a theta burst protocol consisting of two trains of four pulses at 100 Hz, 200 ms apart. The procedure was repeated five times with an interval of 30 s. After theta burst stimulation, LTP was recorded for 60 min. Statistical analyses were performed with 2-way ANOVA.

## Antibodies

Antibody HT-7 (Innogenetics, Gent, Belgium) specifically recognizes human tau, whereas antibody JN-RF.5 (generous gift from M. Mercken) reacts only with murine tau. Antibodies R2 (5) and RD4 (U.S. Biologicals, Swampscott, MA, USA) are specific for the second repeat domain and thereby for tau-4R isoforms. Antibody tau-5 (BD, Brussels, Belgium) detects all tau species. The BrdU antibody (Abcam, Cambridge, UK) detects cells that have passed through the DNA synthesis phase of the cell cycle. Antibodies against nestin (Abcam) and NeuN (Chemicon, Leuven, Belgium) detect nonproliferating precursors and differentiated neurons, respectively. The doublecortin antibody (C-18; Santa Cruz, USA) detects young, migratory neurons. SMI-312 is a mixture of monoclonal antibodies (Sternberger, Lutherville, MD, USA) that stains medium and high molecular weight neurofilaments in axons.

## Immunohistochemistry

All mice were anesthetized and transcardially perfused with ice-cold saline. Brains were immersion fixed in 4% paraformaldehyde for 24 h and then sectioned on vibratome (40  $\mu$ m) or embedded in paraffin and sectioned serially (8 or 10  $\mu$ m).

At P30, mice were injected intraperitoneally with 5 mg/ml BrdU in 0.9% saline at 50 mg/kg for seven consecutive days. Four weeks later, they were sacrificed, and BrdU-labeled nuclei were visualized as described by (16). After quenching, formic acid and HCl treatment, free-floating sections were stained with the BrdU antibody (1:3000, Roche, Switzerland) in phosphate buffer with 0.1% bovine serum albumin (BSA), and 0.3% Triton X-100. Sections were incubated with biotinylated secondary antibody and avidin-biotin complex (ABC) (Vector Laboratories, Amsterdam, The Netherlands). The peroxidase reaction was visualized with DAB/H<sub>2</sub>O<sub>2</sub>.

For doublecortin staining, sections were incubated with primary antibody, 1:1500 in 0.25% gelatin, 0.5% triton-X-100, 0.1 M TBS (Supermix), then with biotinylated secondary antibody (1:200). The avidin-biotin reaction was enhanced by biotinylated tyramide and, amplified with avidin-biotin peroxidase complex. The peroxidase reaction was visualized with DAB/H<sub>2</sub>O<sub>2</sub>. TUNEL staining was performed on 10- $\mu$ m paraffin sections according to (17). At least 4 individual mice were used for each age group and at least 3 or 4 separate sections from each. Statistical analyses were carried out with a 2-way ANOVA.

## Golgi silver impregnation

Golgi staining was performed as described in (15). Briefly, mice were decapitated, brains removed and placed in Golgi-Cox solution. After washing and dehydration in graded alcohols and ether, brains were saturated in celloidine solutions and cut into 200- $\mu$ m coronal sections. Staining was visualized with 16% ammonia and 1% sodium thiosulfate. Dentate granule cells were selected from the middle third of the inner pyramidal blade at bregma -2.54 mm. Pyramidal cells were selected from the same level of the CA1 area opposite to the middle third of the suprapyramidal blade of the DG. If neurons were completely stained and horizontally orientated within the section, 99 Z-stacks of 1  $\mu$ m were recorded with Image-Pro Plus, (Media Cybernetics, Silver Spring, MD, USA), using an Axioplan 2 (Zeiss) microscope, equipped with an Evolution QEi FAST camera (Media Cybernetics), at  $\times$ 40, then analyzed with the drawing tool NeuroDraw (Image-Pro Plus, Netherlands Institute for Brain Re-

search, Amsterdam, The Netherlands) (18). Statistical analyses were performed with the Mann-Whitney *U* test.

## Cell culture

Embryonic hippocampal neuronal cultures were prepared from E17.5 pups according to standard procedure (19, 20). After dissection and tissue dissociation, the cells were seeded on glass coverslips (Menzel-Glaser, Germany) coated with 1 mg/ml poly-L-lysine (Sigma) in 0.1 M borate buffer, pH 8.5, at a density of 100,000 cells/coverslip. Cells were cultured on an astroglial feeder layer in Neurobasal medium (Invitrogen, Merelbeke, Belgium). Some cultures were pulsed with 10  $\mu$ M BrdU (Sigma, USA) for 6 h.

## cDNA constructs and transfection

Tau-3R and tau-4R DNA constructs described in (21) were subcloned into the pcDNA3 vector and transfected into hippocampal cells by electroporation. After tissue dissociation, 10<sup>6</sup> cells were mixed with 10  $\mu$ g DNA in 0.5 ml HBSS (Invitrogen) and electroporated (0.2 kV, 960  $\mu$ F). Cells were plated on glass coverslips coated with 1 mg/ml poly-L-lysine and 10  $\mu$ g/ml laminin (Invitrogen). Transfection rates were quantified by tau immunostaining and ranged between 15–25%.

## Immunocytochemistry

Cells were fixed with 4% paraformaldehyde in 0.1 M phosphate buffered saline (pH 7.4) (PBS). For BrdU staining, cells were treated with 2N HCl. Nonspecific binding was blocked with 10% fetal calf serum in 0.1% Triton-X100 PBS, and cells were stained with primary antibody. Dilutions as follows: HT-7 (1:2,500), JN-RF.5 (1:2,500), BrdU (1:100), nestin (1:1,000), NeuN (1:1,000), SMI-312 (1:10,000),  $\beta$ III-tubulin (1:1000), doublecortin (1:5,000), and MAP-2 (1:1,000). Cells were incubated with biotinylated secondary antibody (1:500), then with avidin-biotinylated peroxidase complex (Vector Laboratories, Burlingame, CA, USA). The peroxidase reaction was developed with DAB/H<sub>2</sub>O<sub>2</sub>. For double labeling, cells were quenched with 3% peroxide, then stained with the second primary antibody with Vector SG or VectaRed as chromogen. TUNEL staining (Promega, Leiden, The Netherlands) was performed according manufacturer's protocol. Microscopy was performed with an Axioplan 2 (Zeiss) microscope. All experiments were repeated on three or more independent cell preparations and cultures, scoring at least 1500 cells per group. Group comparisons were made with the Kruskal-Wallis method and subsequent post hoc tests with the Mann-Whitney *U* test.

## Neurite outgrowth assay

Neurite outgrowth was assayed by culturing the cells in a filter-based compartmentalized culture system, according to manufacturer's instruction (Chemicon). Hippocampal neurons were seeded on laminin coated membrane inserts at a density of 100,000 cells per well in 24-well plate and cultured in Neurobasal medium. The membrane inserts were removed, and the neurites at the opposite side of the membrane were quantified and visualized. Group comparisons were made with the Kruskal-Wallis method, and subsequent post hoc tests with the Mann-Whitney *U* test.

## Western blot analysis

Snap-frozen brain tissue was homogenized in 2 ml of 0.1 M MES buffer (pH 6.4), 0.5 mM MgCl<sub>2</sub>, 1 mM EDTA, 1 mM

EGTA, 1 mM DTT, 0.2 mM PMSF, 20 mM NaF, 0.2 mM Na<sub>3</sub>VO<sub>4</sub>, 1 μM okadaic acid, 5 μg/ml leupeptin, 5 μg/ml pepstatin, 5 μg/ml soybean trypsin inhibitor, 1% sodium deoxycholate, 1% Triton-X-100, and 0.1% SDS. After centrifugation, aliquots of the supernatant brain extract were diluted in Laemmli sample buffer and boiled for 10 min. Cells were lysed in PBS containing 1% Triton X-100, 0.05 mM orthovanadate and complete protease inhibitor mixture (Roche, Belgium). Proteins were separated by SDS-PAGE on 8% Tris-glycine gels (Novex, Zandhoven, Belgium) and Western blotting performed according to standard procedures.

## RESULTS

### Generation and characteristics of Tau-KOKI mice

To replace murine tau expression with that of htau-4R, the thy1-htau-4R/2N recombinant construct was incorporated into a 4-kb genomic fragment previously used to knock out the mouse tau gene completely (12). A single copy of the construct was targeted to exon 1 of the murine tau gene (Fig. 1A) (8, 9). Recombination in ES cells supplied six correctly recombined clones, one of which yielded appreciable coat color chimeras. One male offspring was mated to FVB/N females, and heterozygous breeding was performed for eight generations until homozygous tau-KOKI mice were obtained. Resulting offspring were genotyped by Southern blot analysis and later identified routinely by PCR reactions detecting either the thy-1-tau-4R construct or the unbroken exon 1 of the murine tau gene.

The desired htau-4R expression and complete deficiency of murine tau in tau-KOKI mice were demonstrated by immunohistochemistry and Western blot analysis (Fig. 1B–C). At no time was tau-3R expressed in the tau-KOKI mice. Htau-4R expression was shown to initiate around P12 and reach robust stable levels around P21 (Fig. 1C). The single copy number generated lower expression levels of htau-4R than in the overexpressing tau-4R mice (8), thereby preventing axonopathy and motoric problems (9).

Nontransgenic mice express tau-3R in brain before birth and until around P12, after which tau-4R isoforms become the dominant tau species. Within the hippocampus, tau-3R was found in both cornu ammonis (CA) and dentate gyrus (DG) at P7, but only in the DG at P15 and not at all in brain of older mice (not shown). At P15, tau-4R was expressed in the cortex, basal ganglia, and brain stem of tau-KOKI and nontransgenic mice. The highest levels were found in the hilus and CA3 stratum radiatum (Fig. 1D). The tau-KOKI mice generally expressed lower tau-4R levels than the nontransgenic ones, except for the DG outer molecular layer. Tau expression was very low in the CA1 subfield for both tau-KOKI and nontransgenic mice. Some small cells in DG, CA3, and basal ganglia expressed high somal content of tau-4R in nontransgenic mice; this was not seen in the tau-KOKI mice.

### Increased volume and neuronal cell number in hippocampus of tau-KOKI mice

Up to six months of age, tau-KOKI mice were phenotypically indistinguishable from nontransgenic mice with respect to body weight, behavior, in the home-cage, rearing, grooming, fertility, and litter size. Despite minor differences in tau phosphorylation compared to nontransgenic mice, they developed neither tau pathology nor suffered memory impairment (9), and only late in life did they display some minor motoric and behavioral defects. Consequently, analysis of brain of young and adult tau-KOKI mice by a wide range of histochemical and immunohistochemical staining revealed few differences relative to nontransgenic mice matched for age, gender, and genetic background.

Nissl staining and volumetric analysis did, however, show the hippocampal volume to be increased in adult tau-KOKI mice compared to nontransgenic ones. Unbiased stereological analysis showed that both the volume and neuronal number in the hippocampus of tau-KOKI mice were significantly increased by ~20% (Fig. 2A, B). The increased volume in CA1 ( $P < 0.005$ ) was paralleled by increased numbers of pyramidal cells in CA1 ( $P < 0.001$ ) and of granular cells in the DG ( $P < 0.003$ ). No such volume increases were found in the cerebellum, a brain region with little or no expression of the transgene (Fig. 2C), either in the granular cell layer, the molecular cell layer, or in white matter. Neither did volumetric MRI-analysis performed as in (22) reveal any differences in neocortex or cerebellum size (not shown). From this, we conclude that the neuronal cell number in hippocampal subregions, but not in neocortex or cerebellum, depends on tau-4R expression.

### Increased cell proliferation in hippocampus of tau-KOKI mice

Since increases in hippocampal size and cell number, though not in cell density, were found in the tau-KOKI mice already at 2 mo of age (Fig. 3A–C), the rest of the analyses was performed on mice of that age.

Hippocampal neurogenesis and survival were further assessed by stereological analysis after injection of S-phase marker BrdU and by doublecortin immunostaining for young migrating neurons. BrdU was administered for seven consecutive days from P30 onward, and labeled cells were quantified 4 wk later. The BrdU labeling index (LI) was significantly higher in the subgranular zone (SGZ) of tau-KOKI mice compared to nontransgenic mice ( $P = 0.0005$ ), implying increased survival of nascent cells in the tau-KOKI mice (Fig. 3D, F).

Increased numbers of doublecortin positive cells in the SGZ and the granular cell layer (GCL) of tau-KOKI mice ( $P = 0.0077$  and  $P = 0.024$ , respectively) demonstrated the presence of a young cell population, confirming the increase in proliferation (Fig. 3E, F). Also, TUNEL staining of brain sections of P15 mice demon-

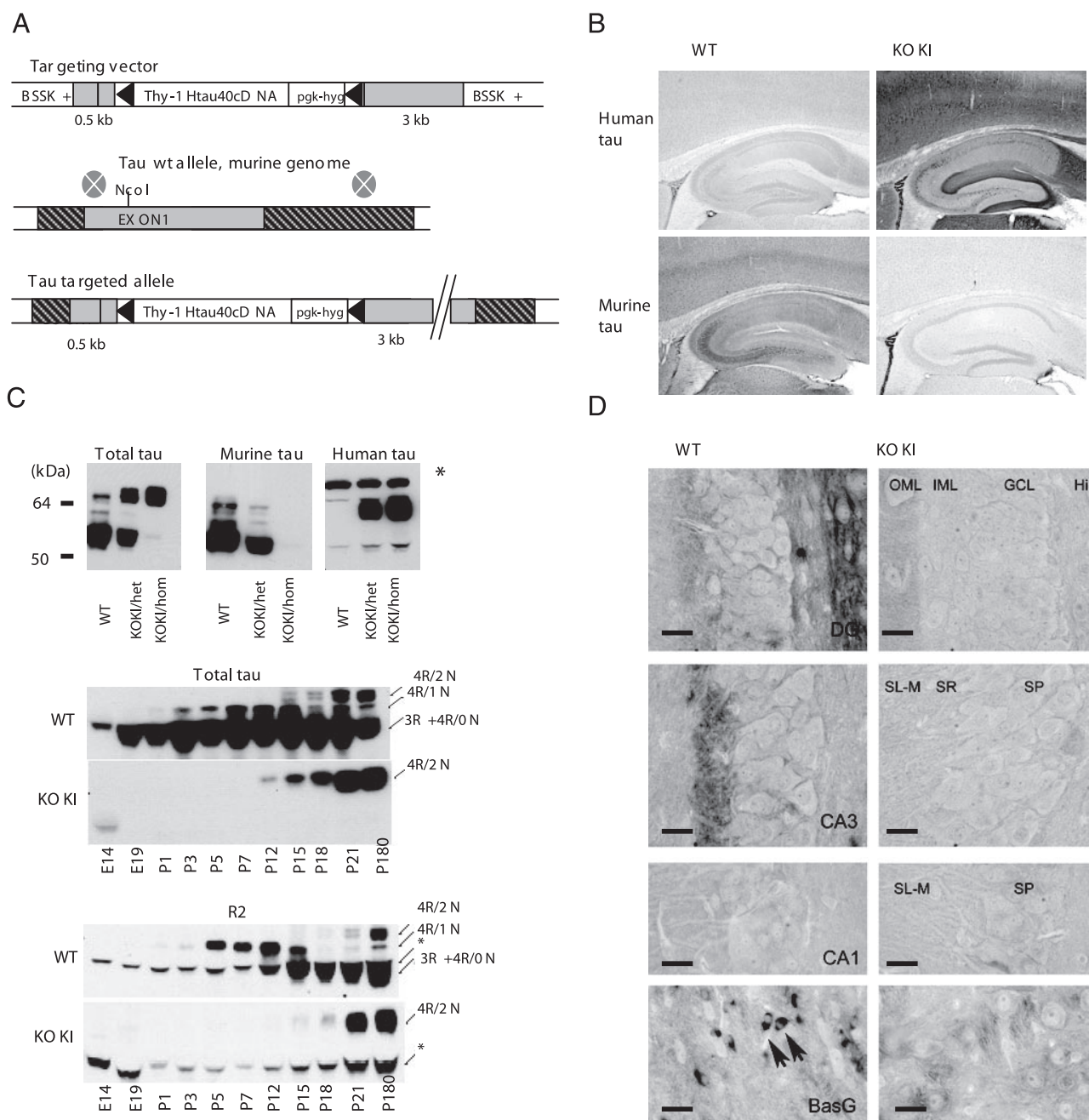


**Figure 1.** Tau expression in tau-KOKI mice. *A*) Schematic representation of recombinant DNA construct (top) used to target exon 1 (gray box) of the mouse tau gene (middle). BSSK+ denotes the pBluescript cloning vector and PKG-hyg the phosphoglycerate-hygromycin gene selection marker. Triangles represent loxP sites. The thy1-tau-4R construct was introduced into the unique *Nco*I restriction site in exon 1 of the tau gene (bottom). *B*) Tau immunohistochemical staining of brain from nontransgenic and tau-KOKI mice at 2 mo of age. Antibody JN-RF.5 stains only murine tau and antibody HT-7 only human tau. *C*) Protein tau in brain extracts from nontransgenic and tau-KOKI mice at 2 mo of age and during a timeline from E14 to P180. Antibody tau5 (total tau), JN-RF.5 (murine tau), HT-7 (human tau) and antibody R2 (tau-4R) in Western blot analysis. Asterisks denote unspecific bands (HT-7 and R2). Nontransgenic (WT), tau-KOKI heterozygous (KOKI/het) and tau-KOKI homozygous (KOKI/hom) mice. *D*) Tau expression in hippocampal subfields DG, CA1, CA3 and basal ganglia (BasG) in tau-KOKI and nontransgenic mice at 1 mo of age. OML, outer molecular layer; IML, inner molecular layer; GCL, granule cell layer; Hil, hilus; SL-M, stratum lacunosum-moleculare; SR, stratum radiatum; SP, stratum pyramidale; BasG, basal ganglia. Scale bar = 10  $\mu$ m

strated less programmed cell death after onset of htau-4R expression in tau-KOKI mice (not shown).

Morphological analysis of dendritic extensions by

Golgi silver impregnation revealed a significant decrease in dendritic arborization in the DG of tau-KOKI mice ( $P=0.001$ ), resulting in less overall space occu-

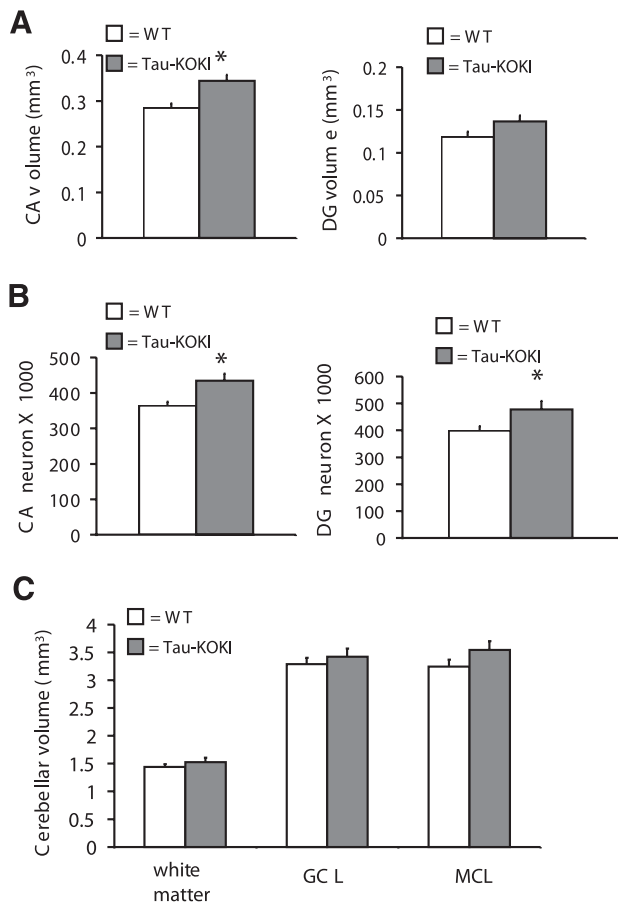


**Figure 2.** Stereological analysis of hippocampus in nontransgenic and tau-KOKI mice at 6 mo of age. *A*) Volume (mm<sup>3</sup>) of CA subregions and DG in tau-KOKI ( $n=7$ ) and nontransgenic mice (WT) ( $n=7$ ). *B*) Number of pyramidal cells in CA subregions and of granular cells in DG in tau-KOKI mice ( $n=7$ ) and nontransgenic mice (WT) ( $n=7$ ). *C*) Volume (mm<sup>3</sup>) of cerebellar white matter, cerebellar granular cell layer (CGL) and cerebellar molecular cell layer (MCL) in tau-KOKI ( $n=7$ ) and nontransgenic mice (WT) ( $n=7$ ). Data are presented as average  $\pm$  SEM with \*  $P \leq 0.05$

pied by individual cells ( $P=0.001$ ) (Fig. 4A–C, G). The number and segment lengths of the dendrites were otherwise similar in tau-KOKI and in nontransgenic mice, only the number of filopodia was decreased in tau-KOKI mice ( $P=0.014$ ) (Fig. 4D–F, G). None of these parameters were altered in the CA1 area, in which tau-4R expression was similar in nontransgenic and tau-KOKI mice (not shown).

These data imply that tau-4R contributes to a mechanism that prolongs the proliferative phase of precursor cells, enhances their survival, and delays their differentiation into the neuronal phenotype. The end result is the establishment of a younger, less differentiated, but more numerous neuronal population in the hippocampi of tau-KOKI mice.

### Improved hippocampal memory retention

Since neurogenesis in the dentate gyrus is an important determinant in hippocampal learning and memory

(23–25), we investigated whether the increased hippocampal size would be paralleled by altered cognitive functions in the tau-KOKI mice. We selected the novel object recognition test (NORT) as a typical and robust hippocampus-dependent task of memory retention in transgenic mice (12, 15, and references therein). NORT depends on short-range visual and tactile stimuli, and the length of delay determines actual hippocampal involvement.

Tau-KOKI mice performed similarly to nontransgenic mice in the 1-h delay NORT. High d2 values indicate that both tau-KOKI and nontransgenic mice remembered the familiar object (Fig. 5A). In the 3.5 h delay NORT, tau-KOKI mice still recognized the familiar object, with d2 values similar to those after 1 h and significantly better than nontransgenic mice ( $P=0.021$ ) (Fig. 5B). This superior memory retention of tau-KOKI mice was observed in two independent sets of experiments in two different cohorts of nontransgenic and tau-KOKI mice at age 9 wk (Fig. 5) and 5 wk (not shown).

Prior to the NORT, the same cohorts of mice were tested for basal sensorimotor parameters by rotarod and open field tests. Tau-KOKI and nontransgenic mice performed equally well in the rotarod test (Fig. 5C). In the open field test, tau-KOKI mice traveled equal distances and spent equal time exploring the objects as nontransgenic mice during the same time interval. Although tau-KOKI mice spent significantly more time in the center, indicating less anxiety ( $P=0.040$ ), (Fig. 5D–E) locomotion, and explorative behavior were not affected.

### Normal LTP in CA1 and DG

To determine cellular and molecular contributions to the improved memory retention, LTP was recorded in the CA1 and DG areas of brain sections from the same cohorts of mice used for immunohistochemistry. Three major determinants, *i.e.*, basal transmission, maximal amplitude or slope, half maximal stimulation intensity and slope factor were not significantly different in either the CA1 or DG of tau-KOKI mice compared to nontransgenic mice (Table 1). No differences were observed in LTP at any time during 1 h of recordings (Fig. 6A–B), indicating that changes in local hippocampal circuit or field properties do not contribute to the improved memory of tau-KOKI mice.

### Tau-4R in primary hippocampal cultures

The contribution of human protein tau to the apparent proliferation and/or neuronal differentiation in the hippocampi of tau-KOKI mice was further examined in primary embryonic hippocampal cultures (E17.5). No htau-4R expression was detectable in tau-KOKI neurons at 4 days in culture (4 DIC) (Fig. 7A, B). Between 4 DIC and 10 DIC, expression of htau-4R increased, reaching stable levels around 10 DIC. The neuronal cultures thus paralleled the timeline of expression of protein tau *in*

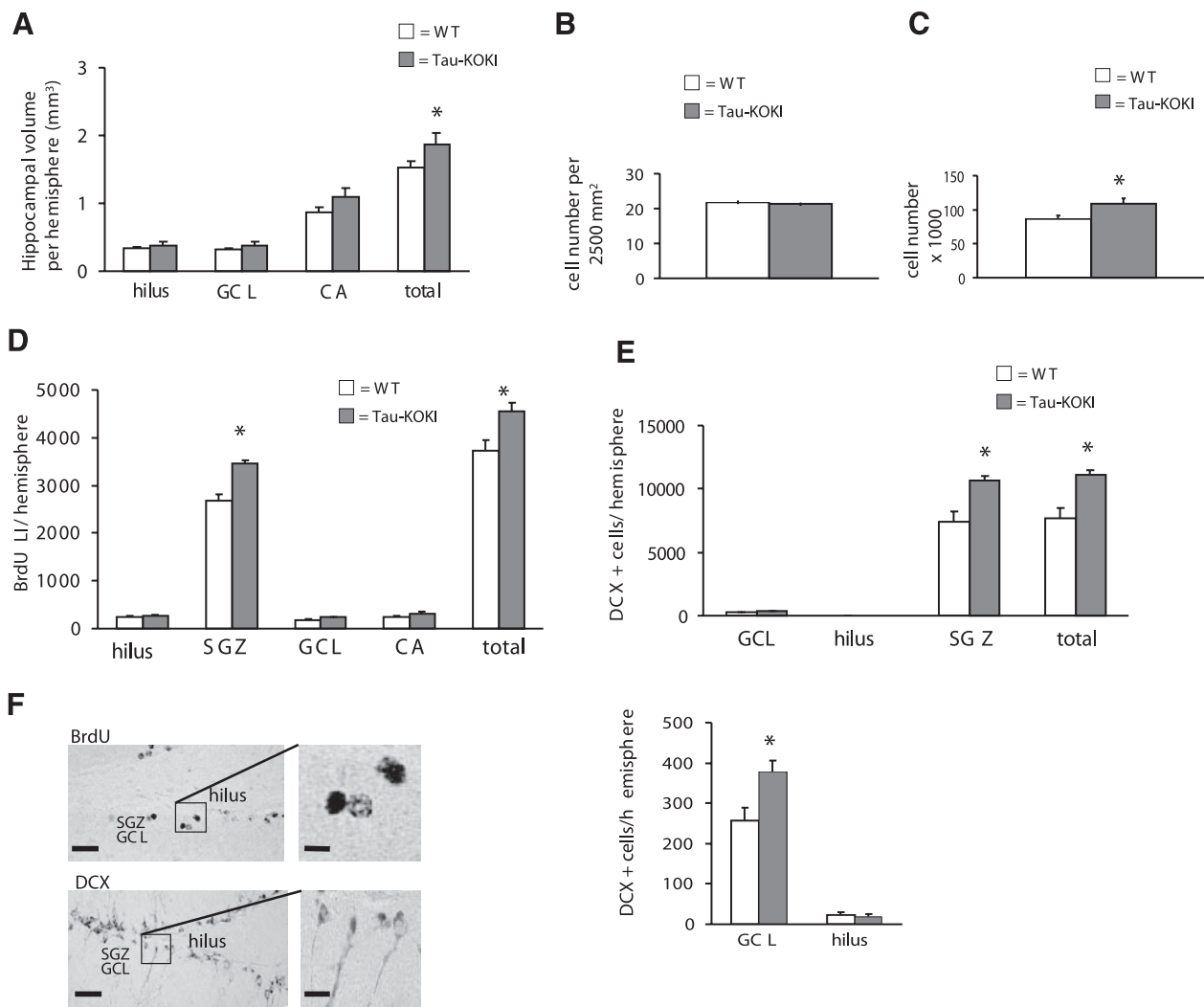


**Figure 3.** Stereological analysis of brain of nontransgenic and tau-KOKI mice at 2 mo of age. *A*) Hippocampal size per hemisphere ( $\text{mm}^3$ ) in tau-KOKI mice ( $n=5$ ) and nontransgenic (WT) mice ( $n=8$ ). Hilus, granular cell layer and CA areas analyzed separately and combined as indicated. *B*) Cell density (cells/ $2500 \text{ mm}^2$ ) in hippocampus of tau-KOKI mice ( $n=7$ ) and nontransgenic (WT) mice ( $n=10$ ). *C*) Total number of hippocampal cells per hemisphere in tau-KOKI mice ( $n=7$ ) and nontransgenic (WT) mice ( $n=10$ ). *D*) Quantitation of BrdU LI in DG of tau-KOKI mice ( $n=8$ ) and nontransgenic (WT) mice ( $n=10$ ). *E*) Quantitation of DCX positive cells in DG of tau-KOKI ( $n=4$ ) mice and nontransgenic (WT) mice ( $n=4$ ). hilus, GCL: granular cell layer, SGZ: subgranular zone. *F*) Representative BrdU and DCX staining of tau-KOKI hippocampus. Large scale bar BrdU =  $50 \mu\text{m}$ . Small scale bar BrdU =  $10 \mu\text{m}$ . Large scale bar DCX =  $80 \mu\text{m}$ . Small scale bar DCX =  $30 \mu\text{m}$ . Data presented as average values  $\pm$  SEM. \* =  $P \leq 0.05$ .

*in vivo*, allowing us to investigate the consequences of 1) absence of tau-3R, 2) initial absence of all tau during early neurodevelopment and 3) expression of human tau-4R in a cell system without confounding effects of other isoforms or endogenous tau.

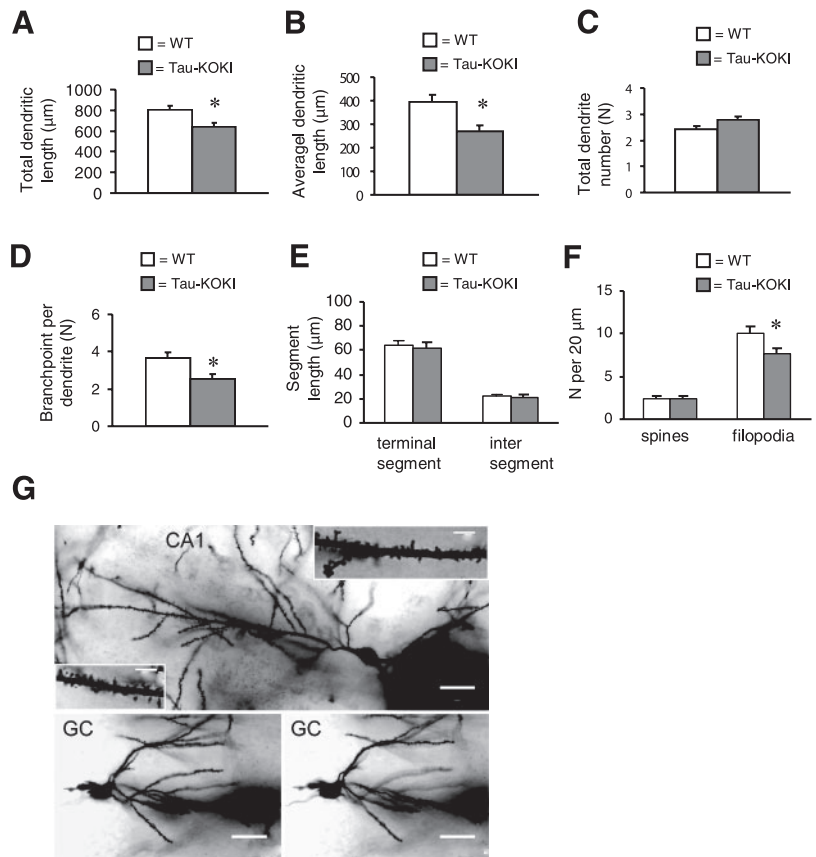
### Neuronal proliferation is suppressed and neuronal differentiation promoted by tau-4R

To define proliferation and neuronal differentiation in the absence and presence of tau, primary cultures were labeled and scored for S-phase marker BrdU and neuronal marker NeuN. At 4 DIC, the BrdU labeling index (LI) was significantly higher ( $P=0.00005$ ) and the ratio of NeuN positive (NeuN+) cells lower ( $P=0.0018$ ) in tau-KOKI cultures compared to nontransgenic ones

(Fig. 7C–D, F). In the absence of protein tau, the population of proliferating precursors (BrdU+ cells) increased and their differentiation into a neuronal phenotype (NeuN+ cells) was delayed.

At 10 DIC, the BrdU LI in the tau-KOKI cultures was reduced to nontransgenic levels, while the ratio of NeuN+ cells was increased ( $P=0.0209$ ). These changes coincided with onset of htau-4R expression, indicating that htau-4R promoted neuronal differentiation. Moreover, staining for precursor marker nestin showed a significantly increased ratio of nonproliferating precursors at 4 DIC ( $P=0.005$ ) and a significantly decreased ratio at 10 DIC ( $P=0.0018$ ) in the tau-KOKI cultures (Fig. 7E, F). TUNEL staining showed cells undergoing programmed cell death in 4 DIC cultures to be less than 10% and in 10 DIC to 12–20%, with no difference

**Figure 4.** Cellular and dendritic parameters of nontransgenic and tau-KOKI mice at 2 mo of age. *A*) Total dendritic length per cell (tau-KOKI:  $n=45$ , WT:  $n=45$ ). *B*) Average dendritic length per cell (tau-KOKI:  $n=45$ , WT:  $n=45$ ). *C*) Total dendrite number per cell (tau-KOKI:  $n=101$ , WT:  $n=91$ ). *D*) Number of branch points per dendrite (tau-KOKI:  $n=101$ , WT:  $n=91$ ). *E*) Average length for interdendrite segments and terminal dendrite segments (tau-KOKI:  $n=41$ , WT:  $n=40$ ). *F*) Average number of spines and filopodia per cell (tau-KOKI:  $n=41$ , WT:  $n=40$ ). *G*) Representative Golgi staining of neurons in CA1 and DG of tau-KOKI mouse (upper panel). Insets: dendritic spines distally (right) and proximally (left) along shaft of apical dendrite of CA1 pyramidal neuron. Bottom panel: two optical sections (out of a stack of 99) recorded of a granule cell (GC). Scale bars = 20  $\mu\text{m}$ . Data are presented as average  $\pm$  SEM with \*  $P \leq 0.05$



between tau-KOKI and nontransgenic cultures (not shown).

These data provide further evidence that absence of tau delayed the neuronal differentiation in a large proportion of precursor cells, allowing the pool of proliferating precursors to expand. Expression of human tau-4R efficiently restored the neuronal differentiation and directed excess precursors toward a neuronal phenotype and fate. The net result is an effective reduction of proliferating precursors to control values, paralleled by an increased number of neurons.

#### Tau-4R promotes axonal and neurite outgrowth

The delayed neuronal maturation and differentiation in tau-KOKI cultures was quantitated in a filter-based compartmentalized culture system. Tau-KOKI primary cells showed significantly less neurite outgrowth at 4 DIC than nontransgenic cultures ( $P=0.0495$ ). Neurite outgrowth of 10 DIC tau-KOKI cells expressing htau-4R did not differ from nontransgenic cells (Fig. 7G). Immunostaining cells with SMI312, specific for axonal phosphorylated neurofilaments, also showed markedly decreased axonal development at 4 DIC, consistent with delayed differentiation in the absence of tau (7H). Again, expression of htau-4R at 10 DIC restored axonal outgrowth. No differences between tau-KOKI and nontransgenic primary cultures were observed for the dendritic marker MAP-2, early neuronal marker doublecortin or  $\beta$ III-tubulin (not shown).

#### The effects of tau-4R are isoform specific

Next, we investigated whether the defective phenotype of tau-KOKI primary cells could be restored to a nontransgenic phenotype of neuronal differentiation at an earlier time point in neuronal development and/or in an isoform-specific mode. To do this, we transfected tau-KOKI primary cells with either htau-3R/2N or htau-4R/2N. Transfected cultures contained comparable number of transfected cells with similar levels of either htau-3R or htau-4R (Fig. 8A).

Tau-KOKI primary cultures transfected with htau-4R, but not with htau-3R, showed a reduced BrdU LI ( $P=0.0495$ ), similar to that of nontransgenic cultures at 4 DIC (Fig. 8B). Similarly, expression of htau-4R, but not htau-3R, restored the ratio of NeuN+ cells in tau-KOKI cultures to that of nontransgenic cultures ( $P=0.0495$ ) (Fig. 8C). Either of the tau isoforms significantly increased neurite outgrowth at 4 DIC ( $P=0.0495$ ) (Fig. 8D), implying that both isoforms overlap largely in their capacity to promote neurite extension and/or stabilization, though the htau-4R generated a three-fold larger increase in neurite protein levels than the htau-3R.

#### DISCUSSION

Protein tau is regarded as a typical microtubule associated protein (MAP) and a neuronal, even axonal

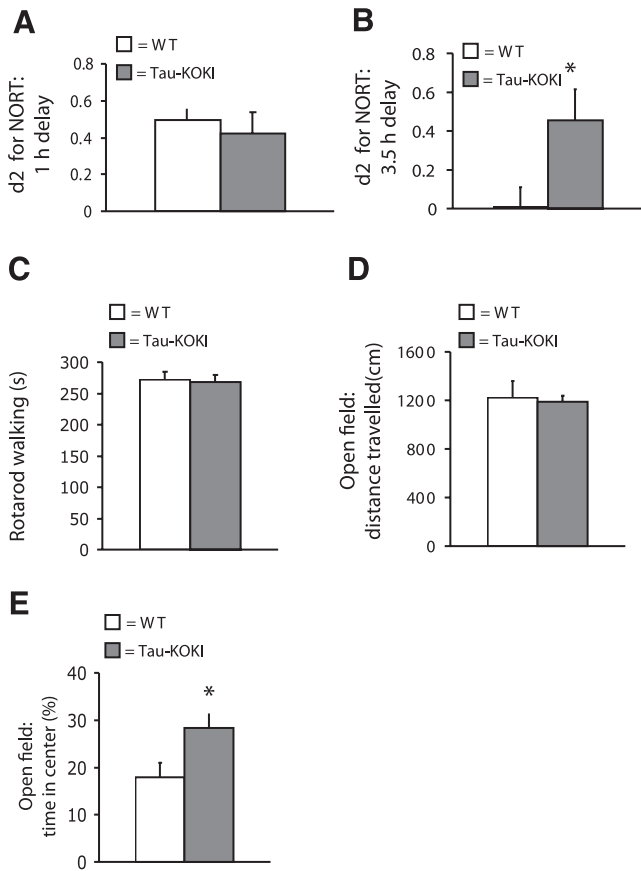


**Figure 5.** Novel object recognition test of nontransgenic and tau-KOKI mice at 2 mo of age. *A*) Novel object recognition discrimination score (d2) after 1-h delay for tau-KOKI mice ( $n=11$ ) and nontransgenic (WT) mice ( $n=13$ ). *B*) Novel object recognition discrimination score (d2) after 3.5 h delay for tau-KOKI mice ( $n=8$ ) and nontransgenic (WT) mice ( $n=13$ ). *C*) Rotarod performance scoring motor function for tau-KOKI mice ( $n=14$ ) and nontransgenic (WT) mice ( $n=11$ ). *D*) Open-field performance scoring locomotor activity in 5 min for tau-KOKI mice ( $n=11$ ) and nontransgenic (WT) mice ( $n=13$ ). *E*) Open field performance scoring explorative behavior for tau-KOKI ( $n=8$ ) and nontransgenic (WT) mice ( $n=13$ ), shown as the time each mouse spent in the center quadrant of the box. Data presented as average  $\pm$  SEM with \*  $P \leq 0.05$

marker. Its precise physiological function in neuronal maturation does, however, remain enigmatic. That tau-deficient mouse strains have been independently

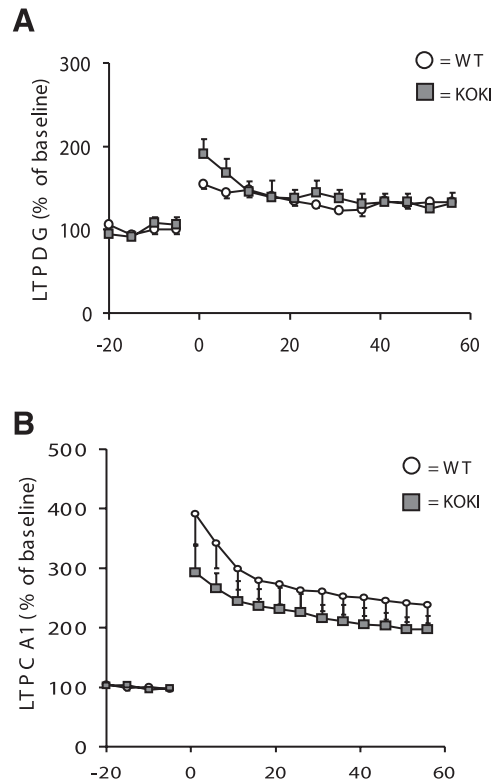


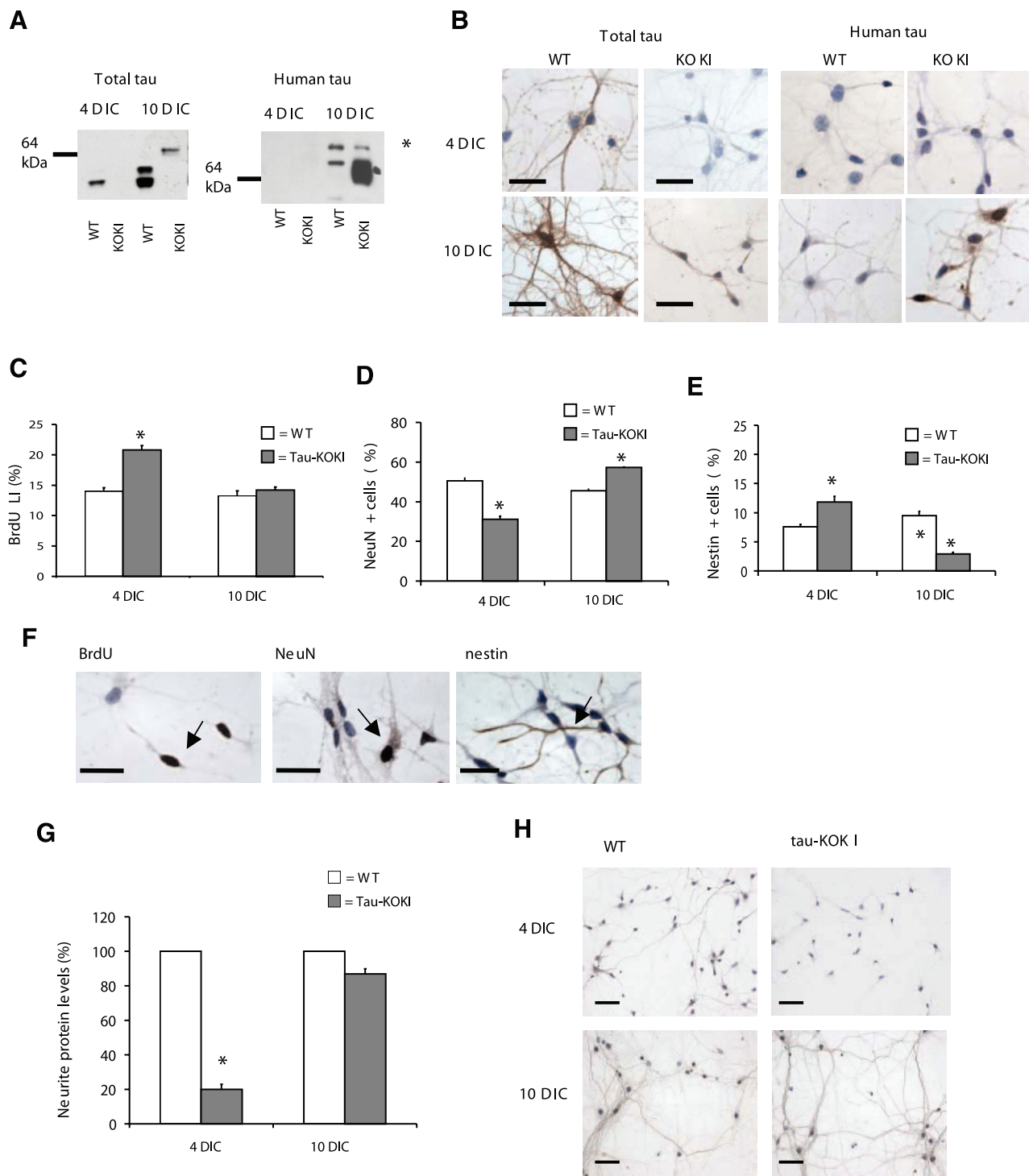
**Figure 6.** LTP in CA1 and DG of nontransgenic and tau-KOKI mice at 2 mo of age. *A*) LTP in DG of tau-KOKI mice ( $n=6$ ) and nontransgenic (WT) mice ( $n=7$ ). *B*) LTP in CA1 of tau-KOKI mice ( $n=12$ ) and nontransgenic (WT) mice ( $n=8$ ). LTP is expressed relative to the average of 20 measurements at  $t = 0$  before theta burst stimulation of LTP. Data are presented as average  $\pm$  SEM with \*  $P \leq 0.05$

generated and characterized as viable, fertile, and lacking major phenotypical defects, strengthens the notion of a considerable functional redundancy in tau function.

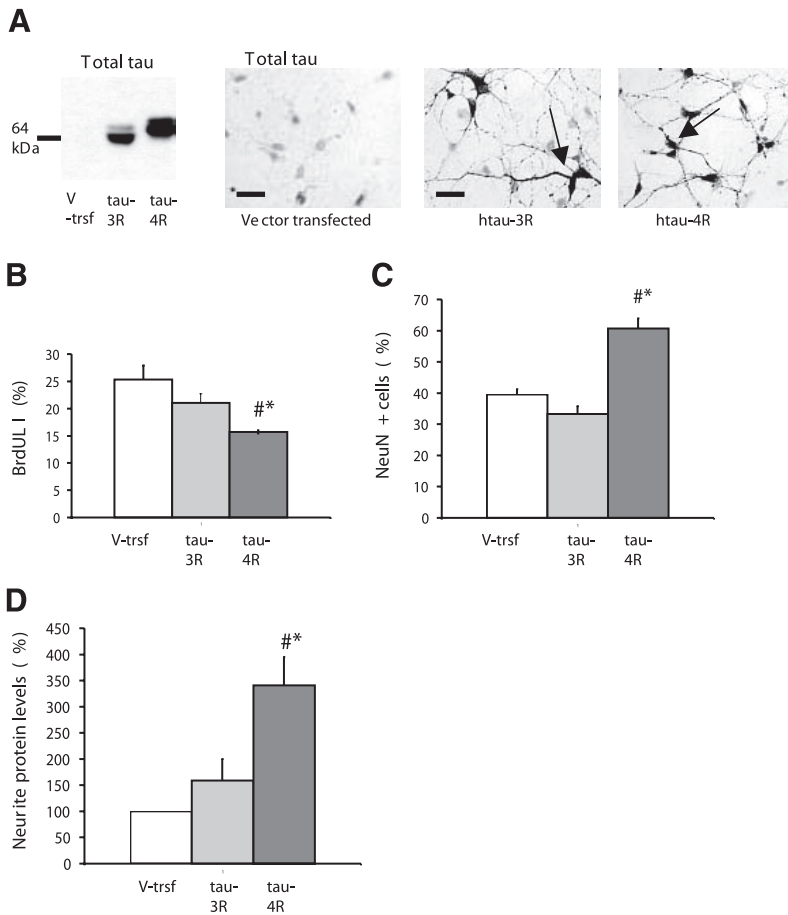
The tau-KOKI mouse was generated as a simplified model expressing only human tau-4R in postnatal neurons in a murine tau-null background. Consistent with the idea of tau being redundant for viability and fertility, tau-KOKI mice evolved normally with only very minor motor and behavior problems at an advanced age (18–24 mo) (9), confirming that mouse brain can develop without tau and undermining an important role for tau-3R isoforms during embryonal and postna-

TABLE 1.

	CA1 (WT)	CA1 (KOKI)	DG (WT)	DG (KOKI)
SLOPE				
$R_{max}$ (mV/ms)	$-2.26 \pm 0.67$	$-3.27 \pm 0.54$	$-1.69 \pm 0.56$	$-1.50 \pm 0.46$
$I_h$ (arbitrary units)	$196 \pm 8.93$	$191 \pm 3.34$	$-197 \pm 3.82$	$191 \pm 0.31$
Slope factor	$-5.99 \pm 1.68$	$-4.90 \pm 1.03$	$-4.13 \pm 0.75$	$-2.58 \pm 0.46$
AMPLITUDE				
$R_{max}$ (mV)	$-3.01 \pm 0.37$	$-2.97 \pm 0.23$	$-1.82 \pm 0.11$	$-1.82 \pm 0.11$
$I_h$ (arbitrary units)	$196 \pm 9.67$	$182 \pm 3.33$	$193 \pm 3.20$	$189 \pm 0.33$
Slope factor	$-6.78 \pm 2.11$	$-5.23 \pm 0.36$	$-4.31 \pm 0.69$	$-4.28 \pm 0.50$



**Figure 7.** Expression of tau and analysis of markers of proliferation, differentiation, and axonal outgrowth in primary hippocampal cultures from tau-KOKI and nontransgenic mice. *A*) Western blot analysis for total tau (antibody tau5) and human tau (antibody HT-7) in cell lysates from nontransgenic (WT) and tau-KOKI primary hippocampal cultures analyzed at 4 and 10 DIC. Asterisks denote unspecific bands reacting with secondary antisera. *B*) Immunocytochemical staining for total tau (tau5) and human tau (HT-7) in nontransgenic (WT) and tau-KOKI primary hippocampal cultures at 4 and 10 DIC. Scale bar = 25  $\mu$ m. *C*) BrdU labeling index (LI) at 4 and 10 DIC. *D*) Ratio of NeuN-positive cells at 4 and 10 DIC. *E*) Ratio of nestin-positive cells at 4 and 10 DIC. *F*) Representative BrdU, NeuN, and nestin staining of primary hippocampal cultures from tau-KOKI mice at 4 DIC. Arrows indicate immunopositive cells. Scale bar = 25  $\mu$ m. *G*) Relative neurite levels of hippocampal cultures at 4 and 10 DIC. *H*) Representative axon-specific staining with antibody SMI-312 of primary hippocampal cultures from tau-KOKI and nontransgenic (WT) mice at 4 and 10 DIC. Scale bar = 100  $\mu$ m. Data are presented as average  $\pm$  SEM with \*  $P \leq 0.05$ .



**Figure 8.** Primary hippocampal cultures from tau-KOKI mice transfected with human tau-3R and tau-4R at 4 DIC. *A*) Western blot analysis for total tau in cell lysates from tau-KOKI primary hippocampal cultures. Vector transfected (V-trsf), htau-3R transfected (tau-3R) and htau-4R (tau-4R) transfected neurons. *B*) Immunocytochemical staining for total tau in vector, htau-3R, and htau-4R transfected E17.5 hippocampal tau-KOKI cell cultures. Scale bar = 25  $\mu$ m. *C*) BrdU-labeling index (LI) in vector, htau-3R, and htau-4R transfected hippocampal tau-KOKI cell cultures. *D*) ratio of NeuN-positive cells in vector, htau-3R, and htau-4R transfected hippocampal tau-KOKI cell cultures. *E*) Relative neurite protein levels in vector, htau-3R, and htau-4R transfected E17.5 hippocampal tau-KOKI cell cultures. Data are presented as average  $\pm$  SEM with \* $P \leq 0.05$  in comparison to vector control values, and # $P \leq 0.05$  in comparison to htau-3R transfected cell values.

tal development. This may be explained by functional overlap with other MAPs (11, 20) or considerable developmental plasticity.

The hippocampus is one of few brain regions to retain the ability to generate neurons throughout life. Neurogenesis in the hippocampus includes proliferation, survival, and differentiation of dentate granule progenitors in the SGZ, which migrate into the GCL, and integrate within existing neuronal circuits. Understanding the developmental profile of newborn granule cells in the neonate and adult is extremely important since the dentate gyrus is a recipient of the perforant pathway and, as such, highly responsive to plastic and pathological changes.

In mice, the generation of hippocampal neurons and formation of the hippocampus are situated in a post-natal window coinciding with the switch in expression from tau-3R to tau-4R (26–28). In tau-KOKI mice, this window also coincides with the onset of expression of the thyl-tau-4R transgene (9, 28). The unexpected observation of a larger hippocampal volume in tau-KOKI mice relative to gender, age, and genetic background-matched nontransgenic mice was shown to be due to a larger number of neurons in CA and DG. Our data demonstrate that survival of BrdU-positive progenitors was significantly higher in tau-KOKI mice after onset of htau-4R expression, while programmed cell death decreased. The corresponding increase in doublecortin positive cells in the SGZ and GCL further

confirmed the increased neurogenesis. Morphologically, neuronal Golgi staining showed less branching of neurites in the DG, indicating a younger, less mature cell population.

The enlarged hippocampal size of tau-KOKI mice was reflected in behavioral tasks, as they performed better than nontransgenic mice in the novel object recognition test. The task depends on hippocampal cognitive capacities, including short-range visual and tactile stimuli. We conclude that increased neurogenesis in the tau-KOKI mice due to the absence of tau is a time-discreet event that nonetheless resulted in enlarged hippocampal volume and improved cognitive capacity.

Using criteria of axonal sprouting and process extension, an important role for protein tau has been suggested in establishing neuronal polarity and formation of contacts and circuits by inhibition with antisense mRNA in primary rat cultures (29) or laser inactivation of labeled tau in chick dorsal root ganglion cultures (30). Primary hippocampal neurons lacking tau were delayed in development of neuronal polarity along with reduced elongation of axons and dendrites, while human tau expression restored sprouting and growth (20). Conversely, hippocampal neurons derived from tau-deficient mice did not show any defects in neuronal maturation, implying that other MAPs compensated for the absence of tau (11, 31). These issues were examined in primary hippocampal cell cultures from tau-

KOKI mice in the absence and presence of human tau-4R. We show that absence of tau delays neuronal differentiation of a large proportion of precursor cells, expanding the pool of proliferating precursors in tau-KOKI cultures compared to nontransgenic cultures. The htau-4R isoform, but not the tau-3R isoform, effectively restored the neuronal differentiation process and subsequently directed the excess precursors toward the neuronal phenotype and fate. Furthermore, the htau-4R isoform is able to rescue the impaired/retarded axonal outgrowth of tau-KOKI-derived primary neuronal cultures. The net result is an effective reduction of the levels of proliferating precursors to control values, concomitant with an increased number of neurons. These observations in cell cultures recapitulate the *in vivo* situation and explain the differential role of tau-3R and tau-4R isoforms.

It has been shown that tau-3R and tau-4R isoforms distinctly affect various parameters of microtubule nucleation and assembly *in vitro* (32, 33). Our results imply additional *in vivo* differences between tau-3R and tau-4R isoforms during development. While tau-3R does not influence cell fate, its assisting of microtubule assembly may allow the generation of a precursor pool. In contrast, tau-4R inhibits proliferation and promotes neuronal differentiation and axonal outgrowth, likely by stabilizing the microtubular network. The postnatal isoform switch to tau-4R may thus be taken as a commitment of precursor cells to a neuronal fate. We suggest that the tau-4R isoform essentially contributes to hippocampal development by controlling proliferation and differentiation of neuronal precursors. FJ

We appreciate and thank N. Hirokawa, H.N. Dawson, K. Spittaels, C. Van den Haute, H. Geerts, L. Umans, L. Serneels, M. Oitzl, J. van Heerikhuize, S. Maslam, P. Borghgraef, H. Devijver and P. Davies for generously providing materials, assistance and expert advice. This study was supported by the Fonds voor Wetenschappelijk Onderzoek-Vlaanderen (FWO), the Instituut voor Wetenschappelijk en Technologisch Onderzoek (IWT), the KULeuven Research Fund, the Rooms-Fund, KULeuven R&D, and by the Internationale Stichting Alzheimer Onderzoek. K.S. is supported by a Marie Curie Fellowship of the European Community (MEIF-CT-2005-010219). K.B. was supported by a predoctoral grant from EURON (Marie Curie Training Site QLK6-CT-2000-60042).

## REFERENCES

- Goedert, M. (1996) Tau protein and the neurofibrillary pathology of Alzheimer's disease. *Ann. N. Y. Acad. Sci.* **777**, 121-131
- Lee, V. M., Goedert, M., and Trojanowski, J. Q. (2001) Neurodegenerative tauopathies. *Annu. Rev. Neurosci.* **24**, 1121-1159
- Buée, L., Bussi re, T., Bu e-Scherrer, V., Delacourte, A., and Hof, P. (2000) Tau protein isoforms, phosphorylation and role in neurodegenerative disorders. *Brain. Res. Rev.* **33**, 95-130
- Larcher, J. C., Boucher, D., Ginzburg, I., Gros, F., and Denoulet, P. (1992) Heterogeneity of Tau proteins during mouse brain development and differentiation of cultured neurons. *Dev. Biol.* **154**, 195-204
- Takuma, H., Shigeki, A., and Mori, H. (2003) Isoform changes of tau protein during development in various species. *Dev. Brain. Res.* **142**, 121-127
- Andorfer, C., Kress, Y., Espinoza, M., de Silva, R., Tucker, K. L., Barde, Y.-A., Duff, K., and Davies, P. (2003) Hyperphosphorylation and aggregation of tau in mice expressing normal human tau isoforms. *J. Neurochem.* **86**, 582-590
- Gotz, J., Streffer, J. R., David, D., Schild, A., Hoernndli, F., Pennanen, L., Kurosinski, P., and Chen, F. (2004) Transgenic animal models of Alzheimer's disease and related disorders: histopathology, behavior and therapy. *Mol. Psych.* **9**, 664-683
- Spittaels, K., Van den Haute, C., Van Dorpe, J., Bruynseels, K., Vandezande, K., Laenen, I., Geerts, H., Mercken, M., Sciot, R., Van Lommel, A., et al. (1999) Prominent axonopathy in the brain and spinal cord of transgenic mice overexpressing four-repeat human tau protein. *Am. J. Pathol.* **155**, 2153-2165
- Terwel, D., Lasrado, R., Snauwaert, J., Vandeweert, E., Van Haesendonck, C., Borghgraef, P., and Van Leuven, F. (2005) Changed conformation of mutant tau-P301L underlies the moribund tauopathy, absent in progressive non-lethal axonopathy of tau-4R/2N transgenic mice. *J. Biol. Chem.* **280**, 3963-3973
- Umans, L., Serneels, L., Lorent, K., Dewachter, I., Tesseur, I., Moechars, D., and F., V. L. (1999) Lipoprotein receptor-related protein in brain and in cultured neurons of mice deficient in receptor-associated protein and transgenic for apolipoprotein E4 or amyloid precursor protein. *Neuroscience* **94**, 315-321
- Harada, A., Oguchi, K., Okabo, S., Kuno, J., Terada, S., Ohsima, T., Sato-Yoshitake, R., Takei, Y., Noda, T., and Hirokawa, N. (1994) Altered microtubule organization in small-calibre axons of mice lacking tau protein. *Nature* **369**, 488-491
- Dewachter, I., Revers , D., Caluwaerts, N., Ris, L., Kuiperi, C., Van den Haute, C., Spittaels, K., Umans, L., Serneels, L., and Thiry, E., et al. (2002) Neuronal deficiency of presenilin 1 inhibits amyloid plaque formation and corrects hippocampal long-term potentiation but not a cognitive defect of amyloid precursor protein [V717I] transgenic mice. *J. Neurosci.* **22**, 3445-3453
- West, M. J. (1993) New stereological methods for counting neurons. *Neurobiol. Aging* **14**, 275-285
- Schmitz, C. (2000) Towards the use of state-of-the-art stereology in experimental gerontology. *Exp. Gerontol.* **35**, 429-431
- Boekhoorn, K., Terwel, D., Biemans, B., Borghgraef, P., Wiegert, O., Ramakers, G. J. A., de Vos, K., Krugers, H., Joels, M., Van Leuven, F., et al. (2006) Improved long-term potentiation and memory function in young Tau-P301L transgenic mice prior to the onset of hyperphosphorylation and tauopathy. (2006) *J. Neurosci.* **26**, 3514-3523
- Heine, V. M., Maslam, S., Joels, M., and Lucassen, P. J. (2004) Prominent decline of newborn cell proliferation, differentiation, and apoptosis in the aging dentate gyrus, in absence of an age-related hypothalamus-pituitary-adrenal axis activation. *Neurobiol. Aging* **25**, 361-375
- Lucassen, P. J., Fuchs, E., and Czeh, B. (2004) Antidepressant treatment with tianeptine reduces apoptosis in the tree shrew hippocampal dentate gyrus and temporal cortex. *Biol. Psych.* **55**, 789-796
- Ramakers, G. J., Winter, J., Hoogland, T. M., Lequin, M. B., Van Hulten, P., Van Pelt, J., and Pool, C. W. (1998) Depolarization stimulates lamellipodia formation and axonal but not dendritic branching in cultured rat cerebral cortex neurons. *Brain. Res. Dev. Brain. Res.* **108**, 205-216
- Banker, G. A., and Cowan, W. M. (1977) Rat hippocampal neurons in dispersed cell culture. *Brain. Res.* **126**, 397-342
- Dawson, H. N., Ferreira, A., Eyster, M. V., Ghoshal, N., Binder, L. I., and Vitek, M. P. (2001) Inhibition of neuronal maturation in primary hippocampal neurons from tau deficient mice. *J. Cell Sci.* **114**, 1179-1187
- Vandebroek, T., Vanhelmont, T., Terwel, D., Borghgraef, P., Lemaire, K., Snauwaert, J., Wera, S., Van Leuven, F., and Winderickx, J. (2005) Identification and isolation of a hyperphosphorylated, conformationally changed intermediate of human protein tau expressed in yeast. *Biochemistry* **44**, 11466-11475
- Spittaels, K., Van den Haute, C., Van Dorpe, J., Terwel, D., Vandezande, K., Lasrado, R., Bruynseels, K., Irizarry, M., Verhoye, M., Van Lint, J., et al. (2002) Neonatal neuronal overexpression of glycogen synthase kinase-3 beta reduces brain size in transgenic mice. *Neuroscience* **113**, 797-808
- van Praag, H., Christie, B. R., Sejnowski, T. J., and Gage, F. H. (1999) Running enhances neurogenesis, learning, and long-

- term potentiation in mice. *Proc. Natl. Acad. Sci. U. S. A.* **96**, 13427–13431
24. Shors, T. J., Townsend, D. A., Zhao, M., Kozorovitskiy, Y., and Gould, E. (2002) Neurogenesis may relate to some but not all types of hippocampal-dependent learning. *Hippocampus* **12**, 578–584
25. Kempermann, G., Wiskott, L., and Gage, F. H. (2004) Functional significance of adult neurogenesis. *Curr. Opin. Neurobiol.* **14**, 186–191
26. Andorfer, C. A., and Davies, P. (2000) PKA phosphorylations on tau: developmental studies in the mouse. *Dev. Neurosci.* **22**, 303–309
27. Goedert, M., Spillantini, M. G., Jakes, R., Rutherford, D., and Crowther, R. A. (1989) Multiple isoforms of human microtubule-associated protein tau: sequences and localization in neurofibrillary tangles of Alzheimer's disease. *Neuron* **3**, 519–526
28. Stanfield, B. B., and Cowan, W. M. (1979) The development of the hippocampus and dentate gyrus in normal and reeler mice. *J. Comp. Neurol.* **185**, 423–459
29. Caceres, A., and Kosik, K. S. (1990) Inhibition of neurite polarity by tau antisense oligonucleotides in primary cerebellar neurons. *Nature* **343**, 461–463
30. Liu, C. W., G., L., and Jay, D. G. (1999) Tau is required for neurite outgrowth and growth cone motility of chick sensory neurons. *Cell Motil. Cytoskel.* **43**, 232–242
31. Takei, Y., Teng, J., Harada, A., and Hirokawa, N. (2000) Defects in axonal elongation and neuronal migration in mice with disrupted tau and map1b genes. *J. Cell Biol.* **150**, 989–1000
32. Utton, M. A., Graham, M. G., Burdett, I. D. J., Anderton, B. H., and Vandecastelle, A. (2001) Functional differences of tau isoforms containing 3 or 4 C-terminal repeat regions and the influence of oxidative stress. *J. Biol. Chem.* **276**, 34288–34297
33. Levy, S. F., LeBoeuf, A. C., Massie, M. R., Jordan, M. A., Wilson, L., and Feinstein, S. F. (2005) Three- and four-repeat tau regulate the dynamic instability of two distinct microtubule subpopulations in qualitatively different manners. *J. Biol. Chem.* **280**, 13520–13528

*Received for publication December 13, 2005.*

*Accepted for publication February 1, 2007.*